Exotic Searches in CMS

Francesco Romeo on Behalf of the CMS Collaboration

Department of Physics and Astronomy, Vanderbilt University, Nashville, TN 37235, USA

Abstract

We provide an overview of the research program dedicated to exploring exotic physics beyond the Standard Model of particle physics within the CMS collaboration. The latest findings from searches for new physics are highlighted, using the most recent dataset collected during the Run 2 period from 2016 to 2018, featuring pp collisions at a center-of-mass energy of 13 TeV and a luminosity of about 138 fb^{-1}. Special attention is devoted to unprecedented investigations, unexplored final states, and innovative analysis techniques aimed at enhancing the discovery potential. These efforts illustrate the CMS experiment's sensitivity across a vast energy range, from $O(1)$ GeV to multi-TeV. No significant deviations from the Standard Model expectations have been observed, although some analyses observed mild excesses, and these results are utilized for constraining various theories that aim to extend the Standard Model.

Keywords: LHC, CMS, exotic searches
DOI: 10.31526/BSM-2023.7

1. INTRODUCTION

The Standard Model (SM) of particle physics successfully explains numerous experimental observations involving weak, electromagnetic, and strong interactions. However, it remains incomplete, failing to account for phenomena such as neutrino masses, matter-antimatter asymmetry, dark matter, and gravity. To address these shortcomings, various theoretical models have been proposed, incorporating additional gauge fields and interactions. While the motivations and implications of these models can vary, they commonly predict the existence of new particles that can be probed at the LHC.

The CMS collaboration has undertaken an extensive and diverse search program to uncover new physics, conducting several analyses using about 138 fb^{-1} of data recorded with its detector [1] from proton-proton (pp) collisions during the Run 2 period in the years 2016 to 2018. The initial focus on straightforward searches for heavy particles has not yielded clear evidence of new physics at the discovery level, despite a few instances where discrepancies between the data and SM predictions have emerged. However, there remains a wide array of possibilities and an expansive phase-space yet to be explored in the pursuit of new physics.

In this proceeding, we provide a summary of recent searches selected based on the following criteria: to demonstrate the CMS experiment's ability to explore a broad phase-space, spanning from low masses at $O(1)$ GeV to multi-TeV scales; to showcase novel experimental strategies and innovative search techniques; and to highlight analyses that reveal mild inconsistencies with the SM using the available dataset, requiring further investigation with additional data. The text below offers a general overview of these searches, emphasizing these aspects without delving into specific analysis details. Readers interested in a comprehensive description of each analysis can refer to the corresponding publications, while all CMS results are available on its scientific webpage [2].

2. SEARCHES AT LOWER MASSES AND COUPLINGS

In this section, we present searches targeting very low masses and couplings, employing diverse strategies that exploit various aspects of physics, along with the development of specialized experimental techniques.

2.1. Search for New Physics Using a Special Trigger Selection

The full details of the analysis outlined in this subsection can be found in [3]. Its objective is to explore the low-mass region by adapting the standard trigger event selection process. In the CMS experiment, events of interest are chosen using a two-tiered trigger system involving custom hardware processors (L1) and dedicated software on CPU processors (HLT), operating at an overall rate of approximately 1 kHz. The bandwidth depends on the number and size of events, allowing for an increase in event rate by reducing their size. This technique, illustrated in Figure 1 (left), is known as the "scouting trigger."

As a physics case, dimuon events selected by the data scouting trigger are recorded to disk with an event size of about 4 kB (8 kB) for data collected in 2017 (2018) at a rate of 0.45 kHz, with a minimum transverse momentum (p_T) threshold down to 3 GeV. This is compared to the size of a standard raw event, which is closer to 1 MB at a rate of 2 kHz, with a minimum p_T of 17 GeV. The trigger efficiency is high, reaching up to about 87%. The two muons are selected requiring $p_\text{T} > 4$ GeV and $|\eta| < 1.9$, identified using a multivariate analysis algorithm, and calibrated using known resonances in the mass range of interest (J/ψ and Upsilon).

The resulting mass distribution, starting from below 1 GeV, is depicted in Figure 1 (right). The signal is extracted by conducting simultaneous signal-plus-background maximum likelihood fits to the dimuon mass distribution, with the main source of systematic uncertainty arising from the mass resolution. No significant excess of events above the expectation from the SM background is

observed. Model-independent limits on the production rates of dimuon resonances within the experimental fiducial acceptance are established, and results are interpreted in the context of a minimal dark photon model and a scenario with two Higgs doublets and an extra complex scalar singlet (2HDM+S).

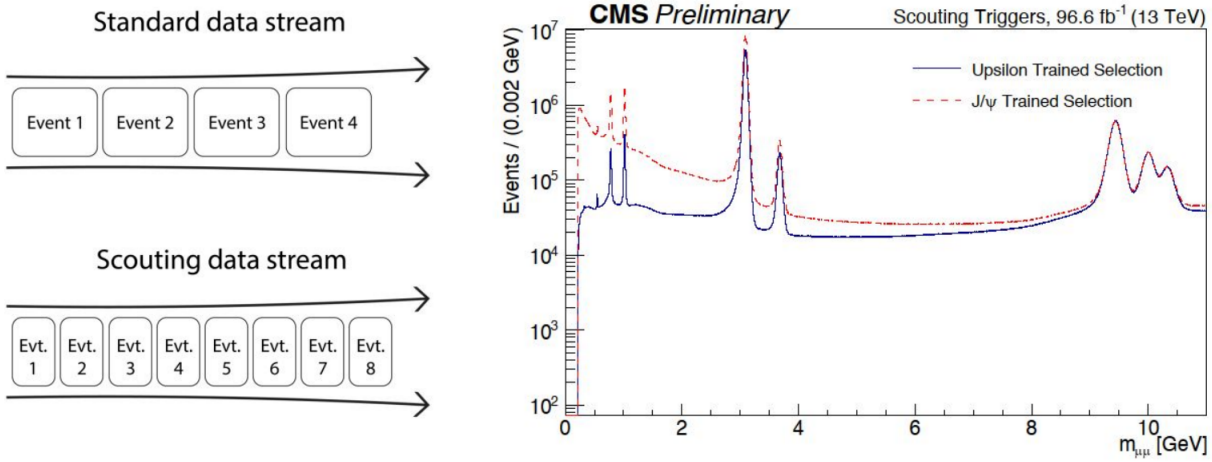

FIGURE 1: *Left*: image depicting the standard trigger data stream, showing a set number of events with a certain size, alongside the scouting trigger data stream, which has a larger number of events with a reduced size, all within the same trigger data bandwidth. *Right*: the dimuon invariant mass distribution obtained from the analysis of muon scouting data, as discussed in [3].

2.2. *Search of New Lorentz-Boosted Resonances*

A different strategy to comply with trigger requirements while accessing an otherwise challenging phase-space, takes advantage of the kinematic constraints of a particle X decaying into two daughters A and B, X $\rightarrow$ AB, as depicted in Figure 2 (left). The angular separation between A and B, denoted by $\Delta R \equiv \sqrt{(\Delta\eta)^2 + (\Delta\phi)^2}$, where η represents the pseudorapidity and ϕ the azimuthal angle, is approximately 2 $\frac{\mathrm{m(X)}}{p_{\mathrm{T}}(\mathrm{X})}$, resulting in a value of around 0.8 (0.4) when p_{T}(X) $>$ 2.5 (5) m(X). This parameter determines the radius to reconstruct a jet, indicating that the products A and B may not be resolved as individual entities but rather as a single object with a multi-prong structure. This characteristic is atypical of the SM background, which is consequently suppressed. The conditions outlined necessitate high p_{T}(X), which can be readily provided in the hadronic environment of the LHC through the emission of a jet (or a photon) with p_{T} (jet/photon) $\sim$ p_{T}(X). Events featuring sufficiently high p_{T} (jet/photon) can meet the required trigger thresholds and occur in conjunction with a Lorentz-boosted particle. This approach has been extensively employed in searches for dijet resonances with masses in the range of O(10–100) GeV, as summarized in Figure 2 (right) and the accompanying references.

2.3. *Search of Long-Lived Particles*

In this subsection, we discuss scenarios involving long-lived particles capable of traversing macroscopic distances within the detector before undergoing decay, resulting in distinct signatures with limited SM background. These particles may appear in the low mass/coupling regime due to mechanisms predicting a suppressed phase space, such as the production and decay of inelastic Dark Matter (DM) states [5] depicted in Figure 3 (top-left), or owing to their lifetime being inversely proportional to mass and width, as for the heavy neutral leptons [6] illustrated in Figure 4 (top-left). A schematic in Figure 3 (top-right) and Figure 4 (top-center) outlines the event signature for these processes within a schematic view of the detector.

Events are triggered based on signal features like missing transverse energy for the DM search or a prompt lepton for the heavy neutrino search. Muon reconstruction necessitates the development of analysis-specific algorithms, posing a significant challenge in these searches and contributing substantially to systematic uncertainties. Background estimation is carried out using a data-driven approach with a modified matrix ("ABCD") method employing two independent variables to discriminate between signal and background, delineating four regions (A–D). Background in the signal-dominated region is constrained based on control regions.

Both searches demonstrate good agreement between observed and expected events. The work in [5] establishes, for the first time at the LHC, an upper limit on the production cross sectionof the inelastic DM process as a function of the mass m_1 of the lighter DM state below 80 GeV and the interaction strength y, as shown in Figure 3 (bottom). The work in [6] sets limits on heavy neutral lepton parameters V_{N_ℓ} across three lepton flavors ($\ell = e, \mu, \tau$), where $V_{\ell N}$ denotes the mixing element between a SM neutrino in its left-handed interaction state and a heavy Majorana neutrino in its mass eigenstate within the Type I Seesaw model. It achieves the most stringent limits to date in the mass range of 2.1–3.0 (1.9–3.3) GeV, with squared mixing parameter values reaching as low as 8.6×10^{-6} (4.6×10^{-6}) in the electron (muon) channel.

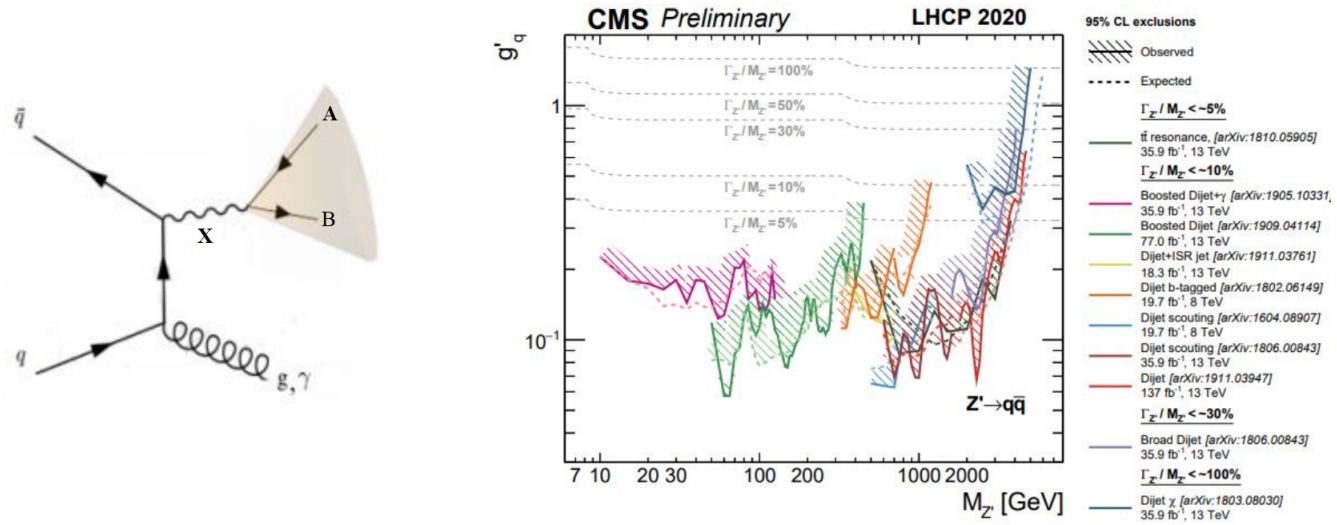

FIGURE 2: *Left*: an illustration of a Feynman diagram showcasing the production of a generic resonance X followed by its decay into two particles A and B, in conjunction with an initial-state radiation gluon or photon. *Right*: observed and expected upper limits at a 95% CL on the universal coupling g'_q between a leptophobic Z' boson and two quarks and its mass. These limits are shown from various CMS dijet analyses, as extracted from [4]. The grey dashed lines show the g'_q values at fixed values of $\Gamma_{Z'}/M_{Z'}$.

2.4. Search for Additional Higgs-Like Particles

Several theories extend the SM and incorporate additional Higgs bosons, including the Two-Higgs Doublet Model (2HDM), the Next-to-Minimal Supersymmetric Model (NMSSM), and models with extra dimensions. In this subsection, we discuss three searches for Higgs-like particles decaying into two photons [7], two taus [9], and two photons plus two bottom quarks [8]. These searches investigate a Higgs-like particle starting from a mass of 50 GeV, and notably, they all exhibit mild discrepancies with the SM expectations for mass hypotheses ranging between approximately 90 and 100 GeV.

In [7], events are selected using a diphoton trigger, and the two offline-selected photons must have a minimum p_T of 18 and 30 GeV, respectively. Additionally, they must pass a machine learning identification based on shape, isolation, energy density, and pseudorapidity variables. Events are further categorized according to different Higgs production modes to enhance the signal significance. Background modeling involves fitting analytic functions to the observed diphoton mass distributions $m_{\gamma\gamma}$ in each event class, with fits performed over the range $60 < m_{\gamma\gamma} < 120$ GeV. An example of such a fit for the entire dataset is shown in Figure 5 (left). The efficiency varies primarily due to the per-photon energy resolution, ranging from 10 to 18%, depending on the year of data collection and the event class. Figure 5 (right) illustrates the observed and expected exclusion limits (95% confidence level) on the product of the production cross sectionand branching fraction into two photons relative to the expected SM-like value for an additional SM-like Higgs boson. The results reveal an excess compared to the standard model prediction, peaking for a mass hypothesis of 95.4 GeV with a local (global) significance of 2.9 (1.3) standard deviations.

The study in [9] look for the presence of heavy neutral Higgs bosons beyond the SM in the final state with two taus and additional b-quark jets, as illustrated in Figure 6 (left). Four main ditau decay products ($\tau_h\tau_h$, $\mu\tau_h$, $e\tau_h$, μe, where τ_h denotes a hadronically decaying tau lepton) are considered. Different categories are defined accounting for the presence of b-quark jets and specific topological requirements, aiming to enhance the signal contribution against the SM background. Background estimation distinguishes between cases with genuine τ lepton pairs and those without. For the former, the "tau-embedding method" is employed, where dimuon events are selected in data, and the muon candidates are replaced with τ_h from simulation. This enables the identification and reconstruction of jets directly from data. For the latter, processes such as QCD multijet, W+jets, and $t\bar{t}$ contribute via jet $\rightarrow \tau_h$ misidentification, and their contribution is estimated by parametrizing the misidentification rate and predicting the number of events from a control region. This procedure entails the highest systematic uncertainty, on the order of tenths of a percentage. Figure 6 (right) displays the distribution of the ditau mass reconstruction using a dedicated reconstruction algorithm that exploits the features of the ditau decays for the event category corresponding to the $\mu\tau_h + e\tau_h$ channel and no b-quark jets. For the low-mass search, the largest deviation from the expectation is observed at a mass of 100 GeV, with a local (global) p-value equivalent to 3.1 (2.7) standard deviations. Within the resolution of the reconstructed invariant mass of the ditau system, this excess aligns with the similar one observed in [8].

The study in [8] investigates the search for a massive particle X decaying either to HH or to H and another spin-0 boson Y, through the process depicted in Figure 7 (left). Events are required to pass a diphoton selection similar to [7], supplemented with the presence of additional b-quark jets. The X candidate, with mass m_X, is reconstructed from the selected pairs of photons and jets. The primary backgrounds arise from SM multijet processes with up to two prompt photons and are mitigated using a boosted decision tree discriminant that incorporates various kinematic and object identification variables. The principal systematic uncertainties include jet energy scale and resolution, b-tagging, and photon selection, which contribute up to 6%. For interpreting

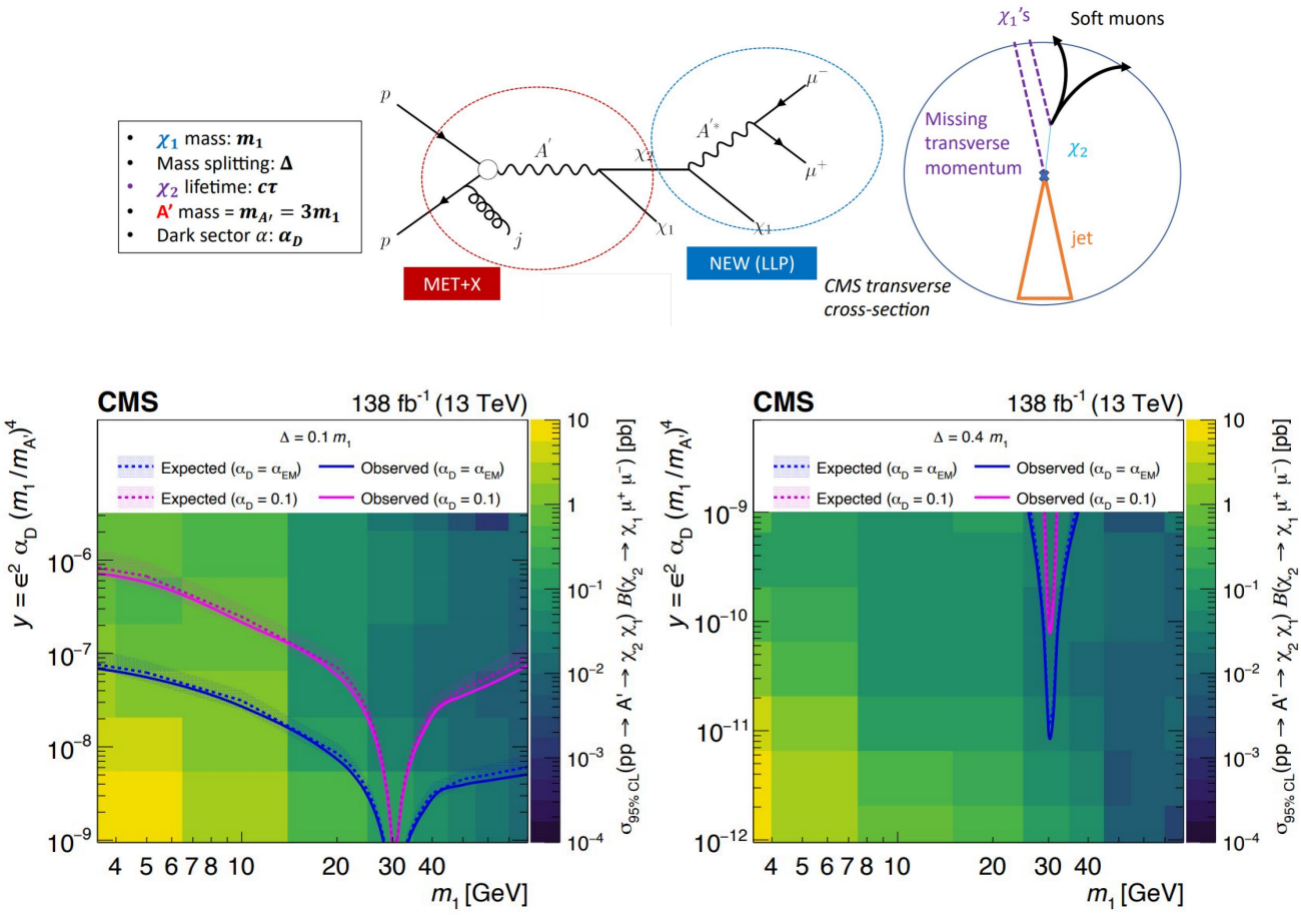

FIGURE 3: *Up*: Feynman diagram illustrating a process of inelastic dark matter production and decay in proton-proton (pp) collisions. Here, the heavier dark matter state χ^2 can exhibit long lifetimes, decaying into χ^1 and a muon pair via an off-shell dark photon A^*. Additionally, a schematic depicts how this signature manifests in the detector. *Down*: two-dimensional exclusion surfaces on $\sigma(pp \to A' \to \chi^1\chi^2) \times \mathrm{Br}(\chi^2 \to \chi^1\mu^+\mu^-)$ for various mass split hypotheses, presented as functions of dark matter mass and interaction strength y, as determined in the search [5].

the results, a likelihood function is constructed using signal and background analytic models of the diphoton and dijet invariant masses. A simultaneous unbinned 2D maximum likelihood fit of their distributions is then executed. Figure 7 presents the expected and observed 95% confidence level exclusion limit on production cross section for the $pp \to X \to HY \to \gamma\gamma b\bar{b}$ signal. The largest deviation from the background-only hypothesis, with a local (global) significance of 3.8 (2.8) standard deviations, is observed for $m_X = 650\,\mathrm{GeV}$ and $m_Y = 90\,\mathrm{GeV}$.

3. SEARCHES AT HIGHER MASSES AND COUPLINGS

In this section, we present findings from searches focusing on high masses and couplings. We summarize investigations about leptoquarks and heavy neutral leptons, highlighting how these analyses have advanced to enhance sensitivity across previously unexplored phase-space.

3.1. Search for Leptoquarks

Leptoquarks (LQs) are theoretical particles that possess both lepton number and baryon number and are predicted in various extensions of the SM aiming to unify fundamental interactions. These extensions include grand unified theories, technicolor models, compositeness scenarios, R-parity violating supersymmetry, and mediators of dark matter-SM interactions. Recently, they have garnered increased attention due to their potential to explain certain observed inconsistencies in $B \to D^*$ transitions and the muon anomalous magnetic moment $(g-2)_\mu$. The CMS collaboration has undertaken an extensive program in the search for LQs, which continues to expand with valuable contributions from the theoretical community. The primary production modes are illustrated in Figure 8. Most analyses focus on LQ pair production (Figure 8(c)) as it is independent of the LQ-lepton-quark vertex λ. However, a novel approach introduced by [10] considers both single LQ (Figure 8(b)) and pair production simultaneously, leveraging the

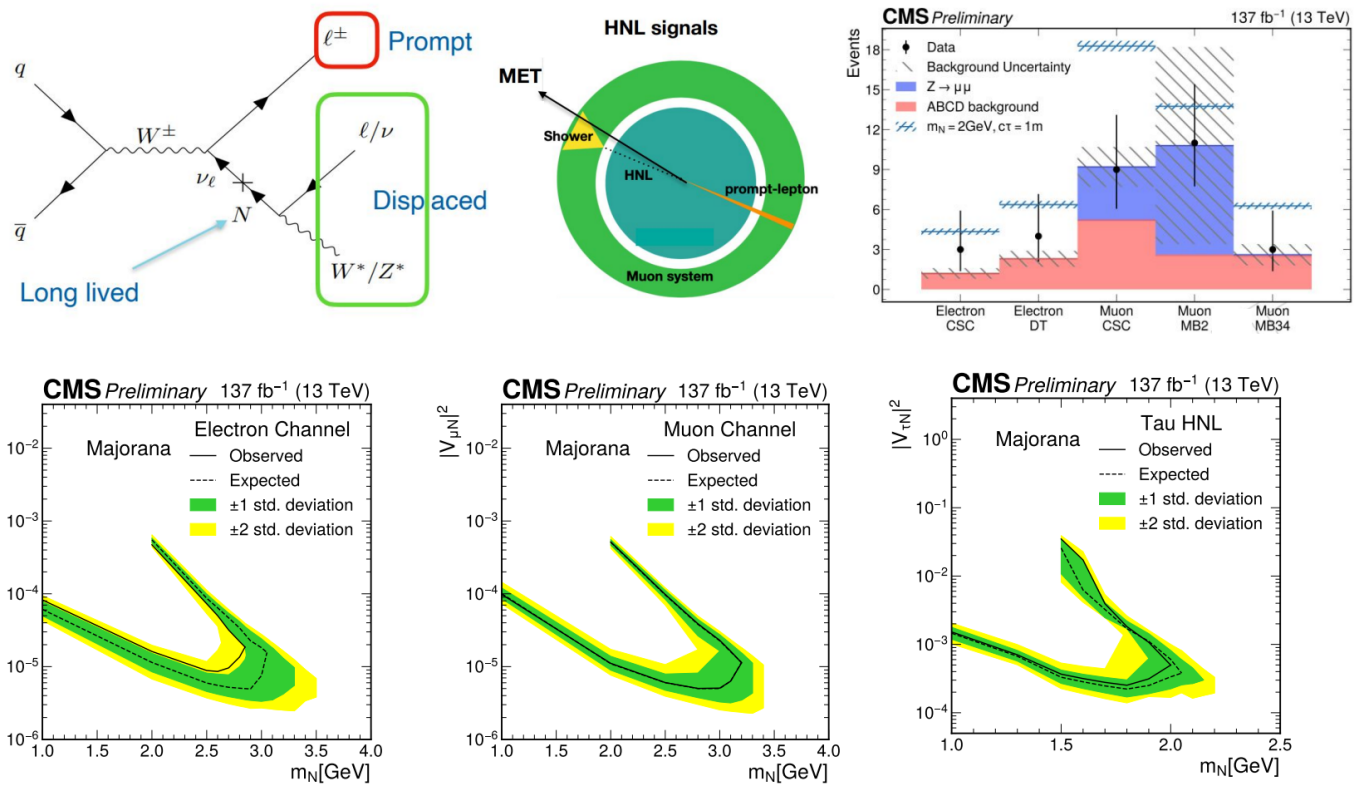

FIGURE 4: *Upper left and center*: Feynman diagram of the Drell-Yan production of a heavy neutral lepton, with emphasis on the prompt and long-lived components (left). A schematic depicts how this signature manifests in the detector (center). *Upper right*: the observed and expected number of events, along with the signal yields of a 2 GeV heavy Majorana neutrino in the signal region, as described in the search [6]. *Down*: the observed and expected upper limits at 95% confidence level on heavy Majorana neutrino production cross-section, presented as functions of its mass and mixing parameter for pure electron (left), muon (center), and tau (right) cases.

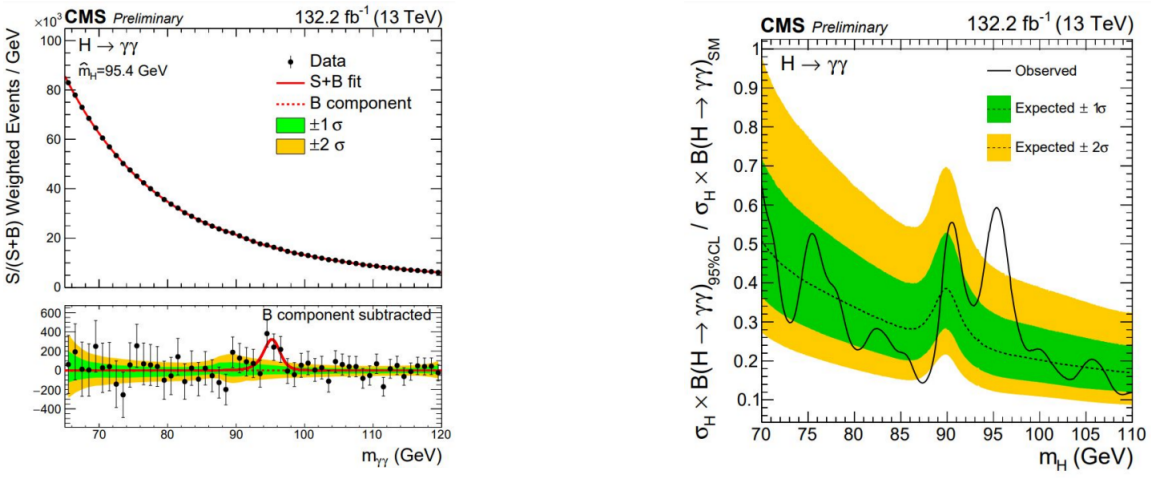

FIGURE 5: *Left*: events weighted by the ratio S/(S+B) across all classes of events of the search in [7], binned as a function of diphoton invariant mass, along with the result of a fit of the signal-plus-background model, for a mass hypothesis of 95.4 GeV. *Right*: observed and expected exclusion limits at 95% confidence level on the product of the production cross section and branching fraction into two photons for an additional SM-like Higgs boson over its prediction from the SM, as reported in [7].

former's enhanced sensitivity due to a cross sectionvarying as a function of λ^2, as highlighted in [11]. More recently, the work in [12] introduced Drell-Yan t-channel production (Figure 8(a)), whose cross section depends on λ^4 and has been identified as a sensitive channel [15]. Furthermore, the work in [14] explored a novel approach utilizing lepton-quark collisions at the LHC (Fig-

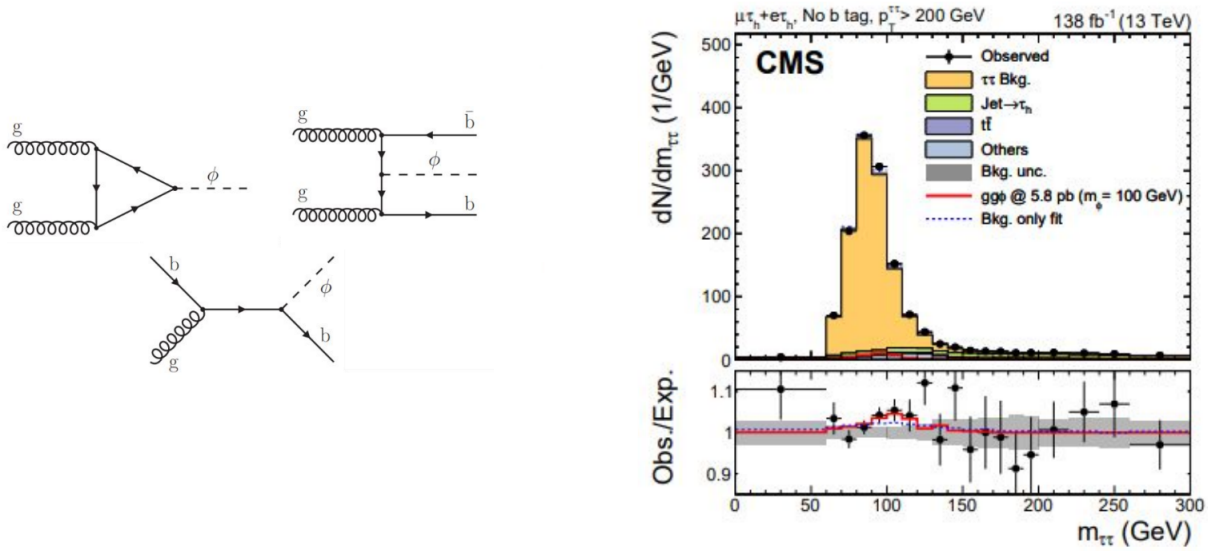

FIGURE 6: *Left*: diagrams illustrating the production of neutral Higgs bosons ϕ through gluon fusion and in association with b quarks. *Right*: distributions of the ditau invariant mass for a specific event category ($\mu\tau_h + e\tau_h$ without b-quark jets). The lower panel displays the ratio of the data to the background expectation after the signal-plus-background fit to the data. These results are sourced from [9].

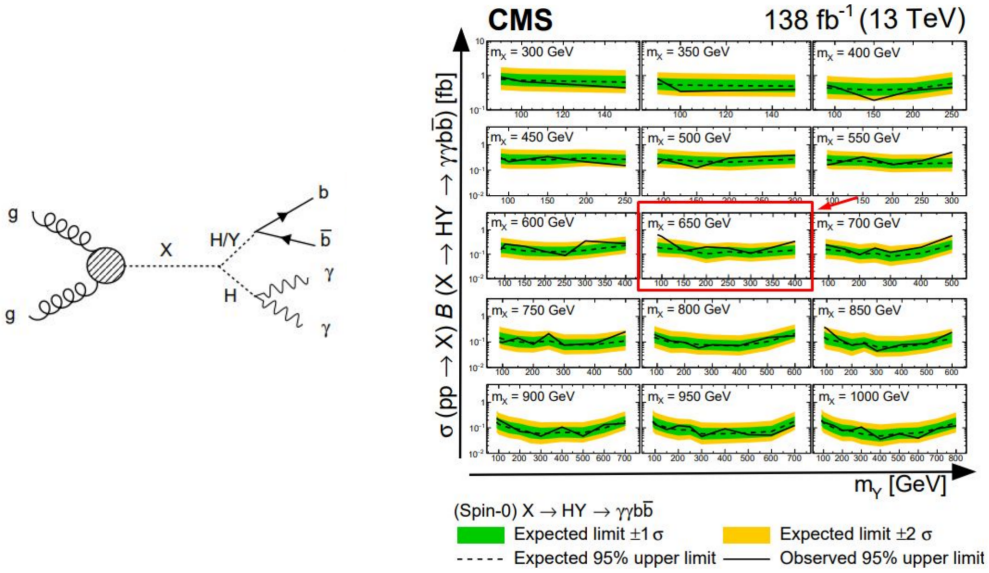

FIGURE 7: *Left*: Feynman diagram illustrating the production of a resonance X beyond the SM, decaying into a pair of spin-0 bosons (HH or HY), which subsequently decay into the $\gamma\gamma b\bar{b}$ final state. *Right*: observed and expected 95% confidence level exclusion limit on the production cross section for $pp \to X \to HY \to \gamma\gamma b\bar{b}$ signal. The middle plot in the third row, highlighted in the red box, displays the highest excess observed for $m_X = 650\,\text{GeV}$ and $m_Y = 90\,\text{GeV}$ in the search [8].

ure 8(d)), a concept proposed decades ago [16] and made feasible in recent years due to advancements in lepton density function understanding [17]. Despite significant progress in LQ searches, new ideas continue to emerge to further enhance sensitivity, as proposed in [18].

Previous analyses predominantly focused on LQ couplings to a lepton and a quark from the third fermion family, which is most pertinent for addressing the aforementioned anomalies. The work in [10] concentrated on the final state comprising a top quark and tau lepton, both decaying hadronically, along with 1 or 2 b-quark jets, to capture single and pair production modes and missing transverse energy. Meanwhile, the work in [12] targeted LQ coupling to a tau lepton and a b-quark, examining the final state with two taus and 0, 1, or 2 jets to probe the production modes in Figures 8(a), 8(b), and 8(c). Additionally, the work in [14] considered the possibility of LQ coupling to a tau lepton and a light-flavor or b-quark jet. In all analyses, background from tau

misidentification as a jet was estimated using a technique akin to that described in [9], while other irreducible backgrounds were constrained through simulation in dedicated control regions.

Overall, all searches exhibited good agreement with the SM prediction and established 95% confidence level LQ exclusion limits in the plane of λ and LQ mass. The outcomes of [10] are depicted in Figure 9, where regions to the left of the lines are excluded. The left plot concerns to a scalar LQ, while the center and right plots represent vector LQ corresponding to Yang-Mills and minimal coupling scenarios defined by the parameter $k = 1$ and 0, influencing LQ interaction with the SM gauge field. The shaded area denotes the parameter space region favored by B physics anomalies according to [11]. The findings of [12] are presented in Figure 10 (left), assuming vector LQ with $k = 0$ and highlighting the region preferred by B physics anomalies from [13]. Notably, in the search for a benchmark LQ model with a mass of 2 TeV and a coupling strength of 2.5, data revealed an excess with a local significance of 2.8 standard deviations above the SM expectation. Additionally, the work in [14] obtained results for the exclusion of LQs coupling to a b quark and a tau lepton (center) and a light-flavor jet and a tau lepton (right) in Figure 10.

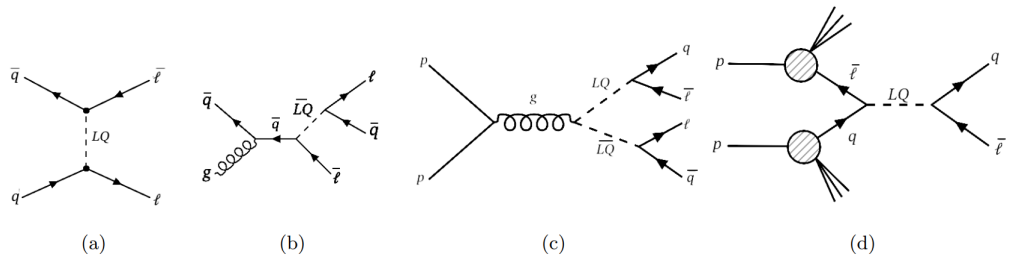

FIGURE 8: Primary Feynman diagrams illustrating the t-channel (a), single (b), pair (c), and lepton-induced (d) leptoquark production modes investigated at the LHC [18].

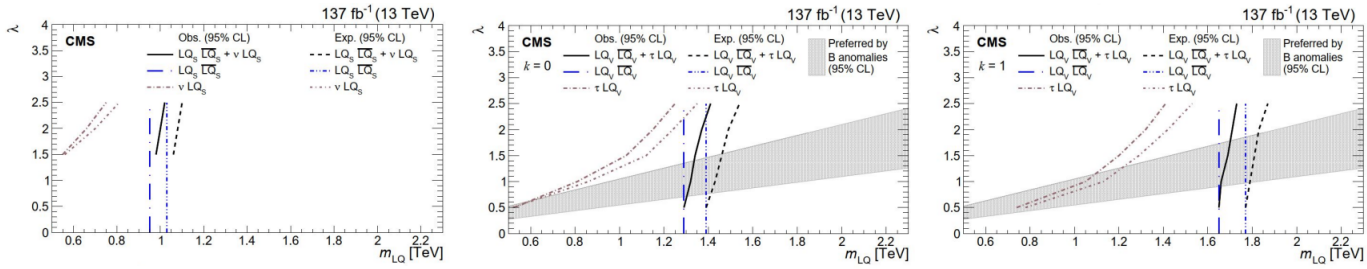

FIGURE 9: Observed and expected 95% confidence level LQ exclusion limits plotted in the plane of the LQ-lepton-quark coupling and its mass. Regions to the left of the lines are excluded. The left plot pertains to a scalar LQ with equal couplings to a top quark and a τ lepton or a b quark and a neutrino lepton, while the lower plots depict a vector LQ with parameter $k = 0$ (center) and 1 (right), featuring equal couplings to a top quark and a neutrino lepton or a b quark and a τ lepton, along with the region preferred by the B physics anomalies for the search in [10].

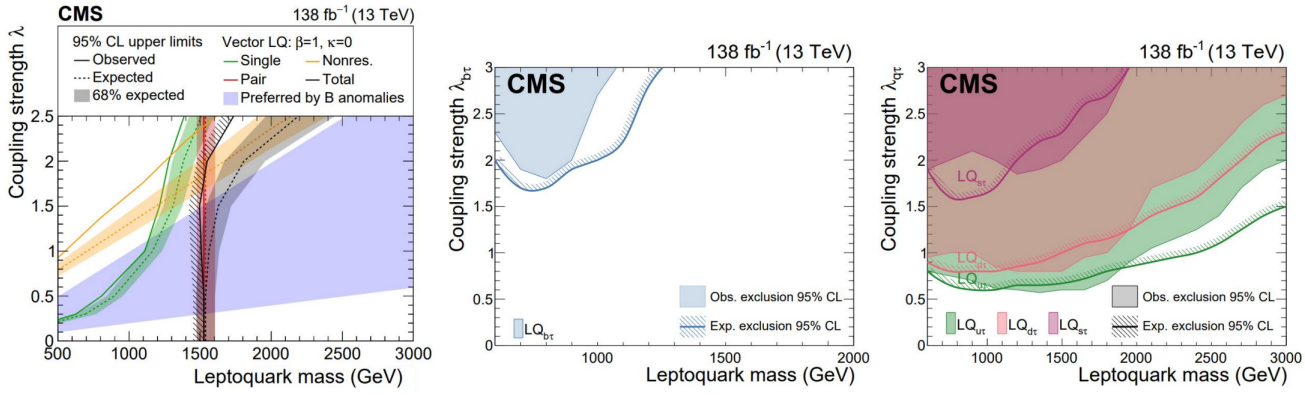

FIGURE 10: *Left*: observed and expected upper limit at the 95% confidence level on the coupling strength λ of a vector LQ model with parameter $k = 0$ coupling to a b quark and a τ lepton, along with the region preferred by the B physics anomalies from the search in [12]. *Center and right*: observed and expected upper limit at 95% confidence level on the coupling strength λ of a scalar LQ to τ leptons and b quark (center) or light-flavor quarks (right) for the search in [14].

3.2. *Search for Heavy Neutrinos*

Search for heavy neutrinos is of utmost importance as the observation of neutrino oscillations has confirmed that they have small, but nonzero, masses. This provides a compelling hint of physics beyond the SM, and several of its extensions foresee mechanisms that point to the existence of new particles at the scale of TeV, which the LHC can probe.

Figure 11 (left) shows the cross sectionover the mixing element parameter $|V_{\ell N}V_{\ell N}|^2$ (WW signal process) or $|V_{\ell N}|^2$ (Drell-Yan and Wγ signal processes) for the production of heavy neutrinos versus their mass. Three mechanisms are highlighted with their corresponding Feynman diagrams: the Drell-Yan and Wγ processes, which are well-known to experimental searches, and the WW scattering process, which has been recently proposed in the literature [19]. The latter mechanism has some interesting features: its cross sectiondominates above a mass of 1 TeV; its signature manifests with two forward jets from vector boson fusion (VBF) and two same-sign leptons, making it very interesting experimentally; it is a t-channel process where the heavy neutrino is non-resonant with the potential to be generated for a mass above the LHC center-of-mass energy.

The investigation in [20] searches for heavy neutrinos based on the WW scattering process described above. It considers a heavy neutrino with muon flavor, and the event selection consists of two same-sign muons plus some requirements typical of the VBF topology with two forward jets with high invariant mass. The main background from nonprompt muons originating from actual jets is estimated directly from a data sample by applying weights to events containing muon candidates that fail the nominal selection criteria while passing a less stringent isolation requirement, with the weights obtained from data. The irreducible background is estimated from simulation constrained using dedicated control regions. The data are found to be consistent with the background expectation. The analysis reports the upper limits at the 95% confidence level on the heavy neutrino production as a function of the mixing element $|V_{\mu N}|^2$ and of the heavy neutrino mass m_N, as shown in Figure 11 (right). The upper limits on the mixing element $|V_{\mu N}|^2$ are set for the mass range $50\,\text{GeV} < m_N < 25\,\text{TeV}$, thus surpassing the center-of-mass energy of the LHC of 13 TeV. The best sensitivity compared to previous searches is reached for $m_N \geq 650\,\text{GeV}$.

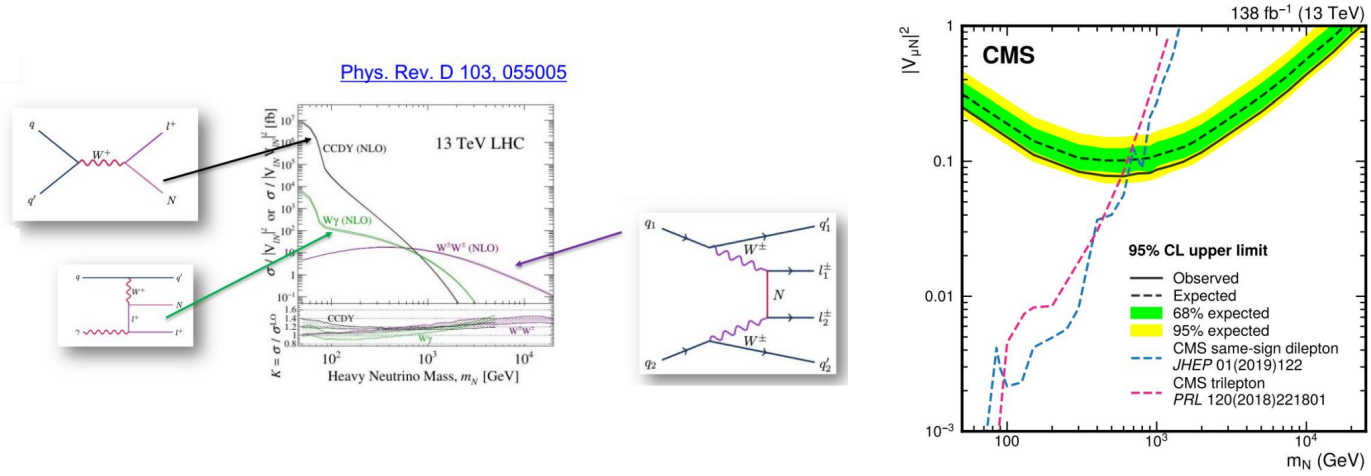

FIGURE 11: *Left*: cross section over the mixing parameter $|V_{\ell N}V_{\ell N}|^2$ (WW signal process) or $|V_{\ell N}|^2$ (Drell-Yan and Wγ signal processes) with respect to mass for a heavy neutrino stemming from the Type I Seesaw model [19]. *Right*: observed and expected upper limits at the 95% confidence level on the heavy neutrino production as a function of the mixing element $|V_{\ell N}|^2$ and of the heavy neutrino mass for the search [20].

4. SUMMARY

In this proceeding, we have summarized some of the most recent searches conducted by the CMS collaboration, encompassing a wide energy spectrum ranging from $O(1)$ GeV up to the multi-TeV scale, extending beyond the most straightforward searches sensitive to the energy regime $O(0.1\text{–}1)$ TeV. Searches at very low masses and couplings rely on four different approaches: scouting trigger, Lorentz-boosted resonances with initial state radiation of a jet or photon, long-lived particles, and additional Higgs-like particles. Searches at very high masses and couplings are pursued based on new ideas from phenomenological studies within the theory community, which impact experimental strategies and allow access to an unprecedented phase-space. Among these searches, some results indicate tensions between observations and the expectations of the SM, requiring further investigation in future analyses with more data. A vast range of possibilities remains open to unveil new physics, and the CMS collaboration continues its quest to explore them.

References

[1] CMS Collaboration, "The CMS experiment at the CERN LHC," JINST **3**, S08004 (2008) doi:10.1088/1748-0221/3/08/S08004.

[2] CMS Collaboration, [https://cms.cern/org/cms-scientific-results].

[3] CMS Collaboration, "Search for direct production of GeV-scale resonances decaying to a pair of muons in proton-proton collisions at $\sqrt{s} = 13$ TeV," JHEP **12**, 070 (2023) doi:10.1007/JHEP12(2023)070 [arXiv:2309.16003 [hep-ex]].

[4] CMS Collaboration, [`https://twiki.cern.ch/twiki/bin/view/CMSPublic/SummaryPlotsEXO13TeV#Moriond\_LHCP\_Fall\_2020`].

[5] CMS Collaboration, "Search for Inelastic Dark Matter in Events with Two Displaced Muons and Missing Transverse Momentum in Proton-Proton Collisions at $s = 13$ TeV," Phys. Rev. Lett. **132**, no.4, 041802 (2024) doi:10.1103/PhysRevLett.132.041802 [arXiv:2305.11649 [hep-ex]].

[6] CMS Collaboration, CMS-EXO-22-017 [https://cds.cern.ch/record/2865227?ln=en].

[7] CMS Collaboration, CMS-PAS-HIG-20-002 [https://cds.cern.ch/record/2852907?ln=en].

[8] CMS Collaboration, "Search for a new resonance decaying into two spin-0 bosons in a final state with two photons and two bottom quarks in proton-proton collisions at $\sqrt{s} = 13$ TeV," [arXiv:2310.01643 [hep-ex]].

[9] CMS Collaboration, "Searches for additional Higgs bosons and for vector leptoquarks in $\tau\tau$ final states in proton-proton collisions at $\sqrt{s} = 13$ TeV," JHEP **07**, 073 (2023) doi:10.1007/JHEP07(2023)073 [arXiv:2208.02717 [hep-ex]].

[10] CMS Collaboration, "Search for singly and pair-produced leptoquarks coupling to third-generation fermions in proton-proton collisions at $s = 13$ TeV," Phys. Lett. B **819**, 136446 (2021) doi:10.1016/j.physletb.2021.136446 [arXiv:2012.04178 [hep-ex]].

[11] D. Buttazzo et al., "B-physics anomalies: a guide to combined explanations," JHEP **11**, 044 (2017) doi:10.1007/JHEP11(2017)044 [arXiv:1706.07808 [hep-ph]].

[12] CMS Collaboration, "Search for a third-generation leptoquark coupled to a τ lepton and a b quark through single, pair, and nonresonant production in proton-proton collisions at $\sqrt{s} = 13$ TeV," [arXiv:2308.07826 [hep-ex]].

[13] C. Cornella et al., "Reading the footprints of the B-meson flavor anomalies," JHEP **08**, 050 (2021) doi:10.1007/JHEP08(2021)050 [arXiv:2103.16558 [hep-ph]].

[14] CMS Collaboration, "Search for scalar leptoquarks produced in lepton-quark collisions and coupled to τ leptons," [arXiv:2308.06143 [hep-ex]].

[15] N. Raj, "Anticipating nonresonant new physics in dilepton angular spectra at the LHC," Phys. Rev. D **95**, no.1, 015011 (2017) doi:10.1103/PhysRevD.95.015011 [arXiv:1610.03795 [hep-ph]].

[16] J. Ohnemus et al., "Single leptoquark production at hadron colliders," Phys. Lett. B **334**, 203–207 (1994) doi:10.1016/0370-2693(94)90612-2 [arXiv:hep-ph/9406235 [hep-ph]].

[17] L. Buonocore et al., "Lepton-Quark Collisions at the Large Hadron Collider," Phys. Rev. Lett. **125**, no.23, 231804 (2020) doi:10.1103/PhysRevLett.125.231804 [arXiv:2005.06475 [hep-ph]].

[18] S. Ajmal et al., "Searching for exclusive leptoquarks with the Nambu-Jona-Lasinio composite model at the LHC and HL-LHC," [arXiv:2311.18472 [hep-ph]].

[19] B. Fuks et al., "Majorana neutrinos in same-sign $W^{\pm}W^{\pm}$ scattering at the LHC: Breaking the TeV barrier," Phys. Rev. D **103**, no.5, 055005 (2021) doi:10.1103/PhysRevD.103.055005 [arXiv:2011.02547 [hep-ph]].

[20] CMS Collaboration, "Probing Heavy Majorana Neutrinos and the Weinberg Operator through Vector Boson Fusion Processes in Proton-Proton Collisions at $s = 13$ TeV," Phys. Rev. Lett. **131**, no.1, 011803 (2023) doi:10.1103/PhysRevLett.131.011803 [arXiv:2206.08956 [hep-ex]].